

# A Double Planetary System around the Evolved Intermediate-Mass Star HD 4732

Bun'ei Sato<sup>1</sup>, Masashi Omiya<sup>1</sup>, Robert A. Wittenmyer<sup>2</sup>, Hiroki Harakawa<sup>1</sup>, Makiko Nagasawa<sup>1</sup>, Hideyuki Izumiura<sup>3,4</sup>, Eiji Kambe<sup>3</sup>, Yoichi Takeda<sup>4,5</sup>, Michitoshi Yoshida<sup>6</sup>, Yoichi Itoh<sup>7</sup>, Hiroyasu Ando<sup>5</sup>, Eiichiro Kokubo<sup>4,5</sup>, and Shigeru Ida<sup>1</sup>

satobn@geo.titech.ac.jp

## ABSTRACT

We report the detection of a double planetary system orbiting around the evolved intermediate-mass star HD 4732 from precise Doppler measurements at Okayama Astrophysical Observatory (OAO) and Anglo-Australian Observatory (AAO). The star is a K0 subgiant with a mass of  $1.7 M_{\odot}$  and solar metallicity. The planetary system is composed of two giant planets with minimum mass of  $m \sin i = 2.4 M_{\text{J}}$ , orbital period of 360.2 d and 2732 d, and eccentricity of 0.13 and 0.23, respectively. Based on dynamical stability analysis for the system, we set the upper limit on the mass of the planets to be about  $28 M_{\text{J}}$  ( $i > 5^{\circ}$ ) in the case of coplanar prograde configuration.

*Subject headings:* stars: individual: HD 4732 — planetary systems — techniques: radial velocities

## 1. Introduction

Precise radial-velocity measurements of stars have revealed more than 500 extrasolar planets in the last 20 years. Thanks to the increase in velocity precision and the duration of the planet search programs, not only single planets but also many multiple-planet systems have been discovered. Around solar-type stars, including those systems with long-term radial-

velocity trends,  $\sim 30\text{--}50\%$  of stars with giant planets are multiple-planet systems (Fischer et al. 2001; Wright et al. 2007, 2009), and systems comprising less massive planets such as super-Earths and Neptune-mass planets are more abundant (Mayor et al. 2011; Howard et al. 2012; Wittenmyer et al. 2011a).

The multiple-planet systems give us deep insights into the formation and evolution of planetary systems (e.g. Ford 2006). For example, evidence of planet-planet scattering events could be preserved in the current orbital configurations of planets (e.g. Ford et al. 2005), and the prevalence of orbital mean-motion resonances constitutes strong support for differential convergent orbital migration having occurred (e.g. Lee and Peale 2002; Kley et al. 2004). Their statistical properties may also provide us hints about the mechanisms of these processes; the rather uniform semi-major axis distribution without the pileup of hot Jupiters and the jump at 1 AU that are seen in single planets, and systematically lower eccentricities compared to single planets (Wright et al. 2009).

<sup>1</sup>Department of Earth and Planetary Sciences, Tokyo Institute of Technology, 2-12-1 Ookayama, Meguro-ku, Tokyo 152-8551, Japan

<sup>2</sup>Department of Astrophysics, School of Physics, University of NSW, 2052, Australia

<sup>3</sup>Okayama Astrophysical Observatory, National Astronomical Observatory of Japan, Kamogata, Okayama 719-0232, Japan

<sup>4</sup>The Graduate University for Advanced Studies, Shonan Village, Hayama, Kanagawa 240-0193, Japan

<sup>5</sup>National Astronomical Observatory of Japan, 2-21-1 Osawa, Mitaka, Tokyo 181-8588, Japan

<sup>6</sup>Hiroshima Astrophysical Science Center, Hiroshima University, Higashi-Hiroshima, Hiroshima 739-8526, Japan

<sup>7</sup>Nishi-Harima Astronomical Observatory, Center for Astronomy, University of Hyogo, 407-2, Nishigaichi, Sayo, Hyogo 679-5313, Japan

Studying the long-term orbital stability of multiple-planet systems is also important. Since the best fit orbital parameters derived from radial-velocity data do not necessarily guarantee that the resulting orbits are stable over long periods of time, dynamical stability analysis can check and further constrain the system parameters, such that the solutions consistent with the data are stable (e.g. Lovis et al. 2006; Pepe et al. 2007; Niedzielski et al. 2009a; Wright et al. 2009; Johnson et al. 2011b; Robertson et al. 2012b; Wittenmyer et al. 2012b).

Here we report the detection of a double giant-planet system around the evolved intermediate-mass star HD 4732 (K0 IV,  $M = 1.7 M_{\odot}$ ), one of the 300 targets of the Okayama Planet Search Program (e.g. Sato et al. 2012). This discovery was facilitated by joint precise radial-velocity observations made from the Anglo-Australian Observatory. Discoveries of planets and multiple-planet systems around such intermediate-mass stars have been rapidly growing in number during the past several years. Although the number of known multiple-planet systems around intermediate-mass stars is still small, it is interesting that many of them appear to be in mean-motion resonances such as 24 Sex (2:1; Johnson et al. 2011b), HD 102272 (4:1; Niedzielski et al. 2009a),  $\nu$  Oph (6:1; Quirrenbach et al. 2011; Sato et al. 2012), and BD20+2457 (3:2; Niedzielski et al. 2009b). Although detailed dynamical studies are required to determine whether these systems are truly in resonance (e.g. Robertson et al. 2012a; Wittenmyer, et al. 2012c), the existence of such systems suggests that the planetary orbital migration process for intermediate-mass stars is similar to that for solar-type ones.

This paper is organized as follows. The stellar properties are presented in section 2 and the observations are described in section 3. Orbital solution are presented in section 4 and results of line shape analysis are described in section 5. Dynamical stability analysis is presented in section 6 and section 7 is devoted to summary.

## 2. Stellar Properties

HD 4732 (HR 228, HIP 3834) is listed in the Hipparcos catalog (ESA 1997) as a K0 giant with the apparent  $V$ -band magnitude  $V = 5.90$  and the

parallax  $\pi = 17.70 \pm 0.99$  mas, giving the distance of  $56.5 \pm 3.2$  pc and the absolute visual magnitude  $M_V = +2.04$  taking into account the correction of interstellar extinction  $A_V = 0.10$  based on Arenou et al. (1992)’s table (Takeda et al. 2008).

Atmospheric parameters (effective temperature  $T_{\text{eff}}$ , surface gravity  $\log g$ , micro-turbulent velocity  $v_t$ , and Fe abundance [Fe/H]) of all the targets for Okayama Planet Search Program were derived by Takeda et al. (2008) based on the spectroscopic approach using the equivalent widths of well-behaved Fe I and Fe II lines of iodine-free stellar spectra. Details of the procedure and resultant parameters are presented in Takeda et al. (2002) and Takeda et al. (2008). For HD 4732, they obtained  $T_{\text{eff}} = 4959$  K,  $\log g$  (cgs) = 3.16,  $v_t = 1.12$  km s<sup>-1</sup>, and [Fe/H] = +0.01 as well as projected rotational velocity of  $v \sin i_{\text{rot}} = 1.45$  km s<sup>-1</sup>.

With use of these atmospheric parameters together with  $M_V$ , a bolometric correction based on the Kurucz (1993)’s theoretical calculation, and theoretical evolutionary tracks of Lejeune & Schaerer (2001), Takeda et al. (2008) also determined luminosity  $L$  and mass  $M$  for HD 4732 to be  $L = 15.5 L_{\odot}$  and  $M = 1.74 M_{\odot}$ . The stellar radius  $R$  was estimated to be  $R = 5.4 R_{\odot}$  using the Stefan-Boltzmann relationship and the measured  $L$  and  $T_{\text{eff}}$ . Although the star is listed in the Hipparcos catalog as a giant star, the star is better regarded as a subgiant rather than giant based on the surface gravity and its position on the HR diagram (Fig 1). The stellar properties are summarized in Table 1.

Hipparcos observations revealed photometric stability for the star down to  $\sigma_{\text{HIP}} = 0.006$  mag. Furthermore, the star shows no significant emission in the core of Ca II HK lines as shown in Figure 2, which suggests that the star is chromospherically inactive. For subgiants like HD 4732, Johnson et al. (2010) reported a typical radial-velocity jitter, which arises from a number of phenomena intrinsic to the star such as granulation, oscillation, and activity, of about 5 m s<sup>-1</sup>. The value is comparable to that of 6 m s<sup>-1</sup> estimated for HD 4732 in section 4.

### 3. Observation

#### 3.1. OAO Observations

Observations of HD 4732 at OAO were made with the 1.88 m telescope and the HIgh Dispersion Echelle Spectrograph (HIDES; Izumiura 1999) from August 2004 to January 2012. A slit width of the spectrograph was set to 200  $\mu\text{m}$  ( $0.76''$ ) corresponding to a spectral resolution ( $R = \lambda/\Delta\lambda$ ) of 67000 by about 3.3 pixels sampling. For precise radial-velocity measurements, we used an iodine absorption cell ( $\text{I}_2$  cell; Kambe et al. 2002), which provides a fiducial wavelength reference in a wavelength range of 5000–5800  $\text{\AA}$ . We have obtained 48 data points of HD 4732 with signal-to-noise ratio  $S/N=60$ –250  $\text{pix}^{-1}$  by an exposure time of 900–1800 sec depending on the weather condition. The reduction of echelle data (i.e. bias subtraction, flat-fielding, scattered-light subtraction, and spectrum extraction) was performed using the IRAF<sup>1</sup> software package in the standard way.

For radial-velocity analysis, we modeled  $\text{I}_2$ -superposed stellar spectra (star+ $\text{I}_2$ ) by the method detailed in Sato et al. (2002) and Sato et al. (2012), which is based on the method by Butler et al. (1996) and Valenti et al. (1995). In the method, we model a star+ $\text{I}_2$  spectrum as a product of a high resolution  $\text{I}_2$  and a stellar template spectrum convolved with a modeled point spread function (PSF) of the spectrograph. We obtain the stellar spectrum by deconvolving a pure stellar spectrum with the spectrograph PSF estimated from an  $\text{I}_2$ -superposed B-star spectrum. We have achieved a long-term Doppler precision of about 4–5  $\text{m s}^{-1}$  over a time span of 9 years. Measurement error was derived from an ensemble of velocities from each of  $\sim 300$  spectral chunks (each  $\sim 3\text{\AA}$  long) in every exposure. We listed the derived radial velocities for OAO data in Table 2 together with the estimated uncertainties.

#### 3.2. AAT Observations

As HD 4732 is near the southern limit for OAO ( $\delta \sim -25^\circ$ ), it is desirable to make observations

from a more southerly site. To improve the phase coverage for HD 4732, in 2010 September we began observing it with the UCLES echelle spectrograph (Diego et al. 1991) at the 3.9-metre Anglo-Australian Telescope (AAT). UCLES achieves a resolution of 45,000 with a  $1''$  slit. An iodine absorption cell provides wavelength calibration from 5000 to 6200  $\text{\AA}$ . The spectrograph PSF and wavelength calibration are derived from the iodine absorption lines embedded on every pixel of the spectrum by the cell (Valenti et al. 1995; Butler et al. 1996). The result is a precision Doppler velocity estimate for each epoch, along with an internal uncertainty estimate, which includes the effects of photon-counting uncertainties, residual errors in the spectrograph PSF model, and variation in the underlying spectrum between the iodine-free template, and epoch spectra observed through the iodine cell. The photon-weighted mid-time of each exposure is determined by an exposure meter. This technique has been successfully used at the AAT by the Anglo-Australian Planet Search (e.g. Tinney et al. 2001, O’Toole et al. 2009, Jones et al. 2010, Tinney et al. 2011a) and the Pan-Pacific Planet Search (Wittenmyer et al. 2011b). All velocities are measured relative to the zero-point defined by the template observation. AAT/UCLES precision velocities are obtained using the *Austral* code (Endl et al. 2000).

We have obtained 19 AAT observations of HD 4732, and an iodine-free template observation was obtained on 2010 Oct 25. Exposure times ranged from 400 to 1200 s, with a resulting  $S/N$  of  $\sim 100$ –200 per pixel each epoch. The AAT data span a total of 636 days, and have a mean internal velocity uncertainty of  $5.0 \text{ m s}^{-1}$ . The data are given in Table 3.

### 4. Orbit Fitting and Planetary Parameters

For candidate multiple-planet systems, and for planet candidates with orbital periods near one year, it is critical to obtain the most complete possible phase coverage, and it is ideal to independently confirm the signal(s) from independent observatories. A recent example is HD 38283b, a  $0.34 M_{\text{Jup}}$  planet with a period  $P = 363.2 \pm 1.6$  days (Tinney et al. 2011b). That planet required 12 years of observations to confirm, and a ro-

<sup>1</sup>IRAF is distributed by the National Optical Astronomy Observatories, which is operated by the Association of Universities for Research in Astronomy, Inc. under cooperative agreement with the National Science Foundation, USA.

bust detection was further aided by the fact that HD 38283 is circumpolar and so could be observed year-round (although at high airmasses below the pole). Another example is HD 159868c, which has a period  $P = 352.3 \pm 1.3$  days (Wittenmyer et al. 2012b), also worryingly close to one year. Again, more than 9 years of AAT data were needed for a secure detection, and the 352-day period was confirmed independently with Keck data over a 4-year span (Wittenmyer et al. 2012b).

Five years of radial-velocity observations of HD 4732 at OAO revealed evidence of a signal with a period near one year ( $\sim 338$  days). Since this star is near the southern limit for OAO, it is only observable for 5 months of the year, resulting in persistent phase gaps which make the confirmation of such a period extremely difficult. AAT observations in 2010-2011 filled in the critical phase gaps and confirmed the orbital period suggested by the OAO data. Continued observations from both telescopes in 2011-2012 have also revealed a second velocity signal, first manifesting as a residual trend, and subsequently as a second, long periodicity.

To fit the two Keplerian signals evident in the HD 4732 data, we first employed a genetic algorithm. This approach has proven useful in previous work where it was necessary to fit highly uncertain orbits with long periods near the total duration of observations (Wittenmyer et al. 2012a,b; Horner et al. 2012). We ran the genetic algorithm for 10,000 iterations, each consisting of 1000 individual trial fits. The best-fit set of parameters is thus the result of  $\sim 10^7$  trial fits. The parameters of the best 2-planet solution obtained by the genetic algorithm were then used as initial inputs for the GaussFit code (Jefferys et al. 1987), a nonlinear least-squares fitting routine. The GaussFit model has the ability to allow the offsets between data sets to be a free parameter. This is important because the radial velocities from OAO and AAT are not absolute radial velocities, but rather are measured relative to the iodine-free stellar template. Each data set thus has an arbitrary zero-point offset which must be accounted for in the orbit-fitting procedure (Wittenmyer et al. 2009). These offsets are  $3.8 \pm 3.2 \text{ m s}^{-1}$  (OAO) and  $-0.1 \pm 3.7 \text{ m s}^{-1}$  (AAT).

For the final orbit fitting, we added radial-velocity jitter in quadrature to the velocity uncer-

tainty of each observation. This jitter arises from a number of phenomena intrinsic to the star, such as granulation, oscillations, and activity (Saar et al. 1998; Wright 2005). As HD 4732 is an evolved star, scaling relations (Kjeldsen & Bedding 1995, 2011) are not applicable. We thus determine the appropriate level of jitter empirically, by performing two-Keplerian fits with varying levels of jitter. On some dates, the AAT recorded multiple consecutive exposures of HD 4732 (Table 3). This provides one way to estimate the jitter: by noting the velocity spread of the multiple exposures. On the four dates which had multiple exposures, the mean velocity spread is  $2.9 \text{ m s}^{-1}$ . This is, however, a lower limit as the timescales of many jitter sources are on the order of hours (granulation) or months (rotation). We also try a range of jitters from  $4\text{--}10 \text{ m s}^{-1}$ , and note the results of the fits in Table 4. The estimation of radial-velocity jitter is quite uncertain, and this is reflected in Table 4, where we see that the amount of added jitter has little effect on the quality of the resulting fit. We adopt a jitter estimate of  $6 \text{ m s}^{-1}$ , as this value brings the reduced  $\chi^2$  of the fit close to unity. The resulting 2-Keplerian planetary parameters are given in Table 5. The uncertainties on the fitted parameters are derived in the usual way, from the covariance matrix of the least-squares fit. The phase gap for planet b has the greatest impact on the uncertainty in  $T_0$  for that planet. As a result, the uncertainty  $\sigma_T = 18.4$  days remains large even though many orbital cycles of planet b have been observed. The two-planet fit has a reduced  $\chi^2$  of 1.05, and the RMS scatter about the fit is  $7.09 \text{ m s}^{-1}$ . Using a stellar mass of  $1.74^{+0.14}_{-0.20} M_\odot$  (Takeda et al. 2008), the planets have minimum masses  $m \sin i$  of  $2.4 \pm 0.3$  (inner planet) and  $2.4 \pm 0.4 M_{\text{Jup}}$  (outer planet).

## 5. Line Shape Analysis

In order to investigate other possible causes of observed radial-velocity variations such as pulsation and rotational modulation rather than orbital motion, spectral line shape analysis was performed with use of high resolution stellar template spectra. Details of the analysis method are described in Sato et al. (2007) and Sato et al. (2002).

At first, two stellar templates were extracted from five star+I<sub>2</sub> spectra at phases with differ-

ent radial-velocity level,  $\sim 40 \text{ m s}^{-1}$  and  $\sim -20 \text{ m s}^{-1}$ , of the observed radial velocities based on the method by Sato et al. (2002). Cross correlation profiles of the two templates were calculated for about 90 spectral chunks ( $4\text{--}5\text{\AA}$  width each) in which severely blended lines or broad lines were not included, and then three bisector quantities were derived for the cross correlation profile for each chunk: the velocity span (BVS), which is the velocity difference between two flux levels of the bisector; the velocity curvature (BVC), which is the difference of the velocity span of the upper half and lower half of the bisector; and the velocity displacement (BVD), which is the average of the bisector at three different flux levels. Here we used flux levels of 25%, 50%, and 75% of the cross correlation profile to calculate the above three bisector quantities, and obtained  $\text{BVS}=3.9\pm 4.7 \text{ m s}^{-1}$ ,  $\text{BVC}=2.4\pm 3.3 \text{ m s}^{-1}$ , and  $\text{BVD}= -57\pm 11 \text{ m s}^{-1}$  for HD 4732 (Figure 5). Both of the BVS and the BVC are identical to zero and the average BVD agrees with the velocity difference between the two templates. Then the cross correlation profiles can be considered to be symmetric and thus the observed radial-velocity variations are best explained by parallel shifts of the spectral lines rather than distortion of them, which is consistent with the orbital-motion hypothesis.

## 6. Dynamical Stability Analysis

We here present dynamical studies of the HD 4732 system. Since the eccentricities of the planets are relatively small and it is thus considered that they probably have not experienced close encounters, we here assume that the both planets share the same orbital plane and are prograde. For the numerical integrations, we use a 4-th order Hermite scheme. Figure 6 shows the one million year evolution of the best-fit two-Keplerian model derived in section 4, for  $i = 90^\circ$  orbits (i.e. planet masses at minimum). The system has two secular eigenfrequencies related with eccentricity,  $11''/\text{yr}$  and  $28''/\text{yr}$ . Accordingly, the planetary pericenter,  $a(1 - e)$ , and apocenter,  $a(1 + e)$ , distances oscillate with the secular timescale of 76000 yr.

For lower inclinations, since the mass increases proportional to  $1/\sin i$ , mutual perturbations become stronger. The stability map in the  $(a, e)$  plane of the outer planet for different values of

$i$  is shown in Fig. 7. Here we plot the stability index  $D = |\langle n_2 \rangle - \langle n_1 \rangle|$  (in  $^\circ/\text{yr}$ ) following Couetdic et al. (2010), which studied stability of HD202206 system using Laskar’s frequency map analysis (Laskar 1990; Laskar et al. 2001). Following the analysis, we calculate an average of mean motion of the outer planet in 1000 Kepler periods ( $\langle n_1 \rangle$ ) and subtract it from an average of mean motion of the same planet obtained in the next consecutive 1000 Kepler periods ( $\langle n_2 \rangle$ ). Through comparison with the five times longer simulations, we find that the system is regular when  $\log_{10} D \leq -3$  (blue to navy), while the system is chaotic when  $\log_{10} D > -1$  (yellow to red). As inclination decreases, the system loses stability. There is no stable area around  $1\sigma$  of the best fitted coplanar orbits for  $i \leq 5^\circ$ . Thus, in the coplanar prograde configuration, we can roughly set the upper limit on the mass of both of the two planets to be about  $28M_{\text{Jup}}$  ( $i > 5^\circ$ ), which falls in the substellar mass regime.

In top left panel of Fig. 7, one can find effects of mean-motion resonances as green vertical incisions. In the case of this system, based on the best-fit values of argument of pericenter, orbits closer to the mean-motion resonances are more unstable. The best-fit solution derived by the radial-velocity data (white cross) sits between the 7:1 and 8:1 mean-motion resonances. From the orbital integration shown in Fig. 6, we have also confirmed that their resonant angles are not librating. We thus conclude that the outer planet is not in the mean-motion resonances of the inner planet.

## 7. Summary

We report the detection of a double planet system around the evolved intermediate-mass star HD 4732 (K0 IV,  $M = 1.7 M_\odot$ ) by precise radial-velocity measurements at OAO and AAO. The system is composed of two giant planets with minimum masses of  $m_2 \sin i = 2.4 M_{\text{J}}$ , orbital period of 360.2 d and 2732 d, and eccentricity of 0.13 and 0.23, respectively. The joint observations of OAO and AAO allowed us to increase the phase coverage of the nearly 1-yr periodicity of the inner planet and detect long-period signal of the second outer planet.

The configuration of the system is similar to those of other multiple-planet systems currently

known: two giant planets in a combination of intermediate- and long-period orbits with relatively low eccentricities. HD 4732 c is the outer most planetary candidate ( $m_p \sin i < 13 M_J$ ) ever discovered around intermediate-mass stars except for those discovered by direct imaging<sup>2</sup>. The period ratio of the two planets is close to 7:1 or 8:1, but dynamical analysis showed that the system is not in the mean-motion resonance and orbits close to mean-motion resonances are unstable in this case.

One million year orbital evolution of the best-fit two-Keplerian model in a coplanar prograde configuration showed no significant changes in eccentricities, but showed their slight oscillations with secular timescale of 76000 yr. Based on the dynamical stability analysis, we found that the system is dynamically unstable in the case of  $i \leq 5^\circ$  for a coplanar prograde configuration. Thus, we can set the upper limit on the mass of both of the two planets to be about  $28 M_J$  ( $i > 5^\circ$ ) in this case, which falls well into the substellar mass regime.

This research is based on data collected at Okayama Astrophysical Observatory (OAO), which is operated by National Astronomical Observatory of Japan, and at the Anglo-Australian Observatory. We are grateful to all the staff members of OAO for their support during the observations. We thank students of Tokyo Institute of Technology and Kobe University for their kind help for the observations. BS was partly supported by MEXT's program "Promotion of Environmental Improvement for Independence of Young Researchers" under the Special Coordination Funds for Promoting Science and Technology, and by Grant-in-Aid for Young Scientists (B) 20740101 from the Japan Society for the Promotion of Science (JSPS). RW is supported by a UNSW Vice-Chancellor's Fellowship. MN is supported by Grant-in-Aid for Young Scientists (B) 21740324 and HI is supported by Grant-In-Aid for Scientific Research (A) 23244038 from JSPS.

This research has made use of the SIMBAD database, operated at CDS, Strasbourg, France.

<sup>2</sup> $\nu$  Oph c ( $m \sin i = 27 M_J$ ,  $a=6.1$  AU; Sato et al. 2012) is the outer most brown-dwarf companion ever discovered around intermediate-mass stars by radial velocity measurements.

## REFERENCES

- Arenou, F., Grenon, M., & Gomez, A. 1992, *A&A*, 258, 104
- Barnes, R. & Quinn, T. 2004, *ApJ*, 611, 494
- Butler, R. P., Marcy, G. W., Williams, E., McCarthy, C., Dosanjuh, P., & Vogt, S. S. 1996, *PASP*, 108, 500
- Couetdic, J., et al. 2010, *A&A*, 519, A10
- Diego, F., Charalambous, A., Fish, A. C., & Walker, D. D. 1990, *Proc. Soc. Photo-Opt. Instr. Eng.*, 1235, 562
- Endl, M., Kürster, M., & Els, S. 2000, *A&A*, 362, 585
- ESA. 1997, *The Hipparcos and Tycho Catalogues* (ESA SP-1200; Noordwijk: ESA) *A&A*, 394, 5
- Fischer, D. A., Marcy, G. W., Butler, R. P., Vogt, S. S., Frink, S., & Apps, K. 2001, *ApJ*, 551, 1107
- Ford, E.B., Lystad, V., & Rasio, F.A. 2005, *Nature*, 434, 873
- Ford, E. B. 2006, *New Horizons in Astronomy: Frank N. Bash Symposium* 352, 15.
- Howard, A. W., Marcy, G. W., Bryson, S. T., et al. 2012, *ApJS*, 201, 15
- Horner, J., Wittenmyer, R. A., Hinse, T. C., & Tinney, C. G. 2012, *MNRAS*, 425, 749
- Izumiura, H. 1999, in *Proc. 4th East Asian Meeting on Astronomy*, ed. P.S. Chen (Kunming: Yunnan Observatory), 77
- Jefferys, W. H., Fitzpatrick, M. J., & McArthur, B. E. 1987, *Celestial Mechanics*, 41, 39
- Johnson, J.A., et al. 2010, *PASP*, 122, 905
- Johnson, J.A., et al. 2011, *ApJS*, 197, 26
- Johnson, J.A., et al. 2011, *AJ*, 141, 16
- Jones, H. R. A., Butler, R. P., Tinney, C. G., et al. 2010, *MNRAS*, 403, 1703
- Kambe, E., et al. 2002, *PASJ*, 54, 865

- Kjeldsen, H., & Bedding, T. R. 1995, *A&A*, 293, 87
- Kjeldsen, H., & Bedding, T. R. 2011, *A&A*, 529, L8
- Kley, W., Peitz, J., & Bryden, G. 2004, *A&A*, 414, 735
- Kurucz, R. L. 1993, Kurucz CD-ROM, No. 13 (Harvard-Smithsonian Center for Astrophysics)
- Laskar, J. 1990, *Icarus*, 88, 266
- Laskar, J., & Robutel, P. 2001, *CeMDA*, 80, 39
- Lee, M.H. & Peale, S.J. 2002, *ApJ*, 567, 596
- Lejeune, T., & Schaerer, D. 2001, *A&A*, 366, 538
- Lovis, C. et al. 2006, *Nature*, 441, 305
- Mayor et al. 2011, *A&A* submitted (arXiv:1109.2497v1)
- Niedzielski, A., Gozdziewski, K., Wolszczan, A., Konacki, M., Nowak, G., & Zielinski, P. 2009a, *ApJ*, 693, 276
- Niedzielski, A., Nowak, G., Adamow, M., & Wolszczan, A. 2009b, *ApJ*, 707, 768
- O’Toole, S. J., Jones, H. R. A., Tinney, C. G., et al. 2009, *ApJ*, 701, 1732
- Pepe, F. et al. 2007, *A&A*, 462, 769
- Quirrenbach, A., Reffert, S., & Bergmann, C. 2011, *AIPC*, 1331, 102
- Robertson, P., Endl, M., Cochran, W. D., et al. 2012a, *ApJ*, 749, 39
- Robertson, P., Horner, J., Wittenmyer, R. A., et al. 2012b, *ApJ*, 754, 50
- Saar, S. H., Butler, R. P., & Marcy, G. W. 1998, *ApJ*, 498, L153
- Sato, B., Kambe, E., Takeda, Y., Izumiura, H., & Ando, H. 2002, *PASJ*, 54, 873
- Sato, B., et al. 2007, *ApJ*, 661, 527
- Sato, B., et al. 2012, *PASJ* in press (arXiv:1207.3141v1)
- Takeda, Y., Ohkubo, M., & Sadakane, K. 2002, *PASJ*, 54, 451
- Takeda, Y., Sato, B., & Murata, D., 2008, *PASJ*, 60, 781
- Tinney, C. G., Butler, R. P., Marcy, G. W., et al. 2001, *ApJ*, 551, 507
- Tinney, C. G., Butler, R. P., Jones, H. R. A., et al. 2011a, *ApJ*, 727, 103
- Tinney, C. G., Wittenmyer, R. A., Butler, R. P., et al. 2011b, *ApJ*, 732, 31
- Valenti, J. A., Butler, R. P. & Marcy, G. W. 1995, *PASP*, 107, 966.
- Wittenmyer, R. A., Endl, M., Cochran, W. D., Levison, H. F., & Henry, G. W. 2009, *ApJS*, 182, 97
- Wittenmyer, R. A., Tinney, C. G., Butler, R. P., et al. 2011a, *ApJ*, 738, 81
- Wittenmyer, R. A., Endl, M., Wang, L., Johnson, J. A., Tinney, C. G., & O’Toole, S. J. 2011b, *ApJ*, 743, 184
- Wittenmyer, R. A., Horner, J., Marshall, J. P., Butters, O. W., & Tinney, C. G. 2012a, *MNRAS*, 419, 3258
- Wittenmyer, R. A., Horner, J., Tuomi, M., et al. 2012b, *ApJ*, 753, 169
- Wittenmyer, R.A., Horner, J., & Tinney, C.G. 2012c, *ApJ*, submitted
- Wright, J. T. 2005, *PASP*, 117, 657
- Wright, J. T., et al. 2007, *ApJ*, 657, 533
- Wright, J.T., Upadhyay, S., Marcy, G.W., Fischer, D.A., Ford, E.B., & Johnson, J.A. 2009, *ApJ*, 693, 1084

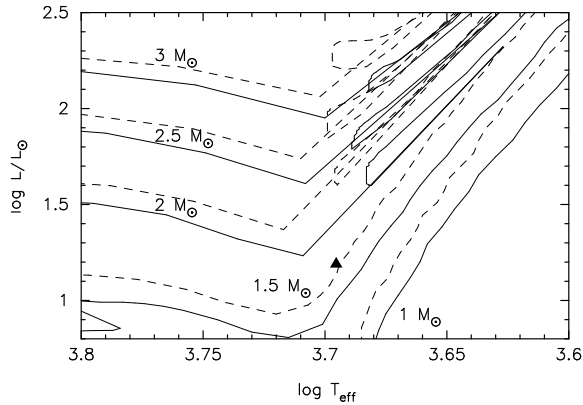


Fig. 1.— HR diagram for HD 4732. Pairs of evolutionary tracks from Lejeune and Schaerer (2001) for stars with  $Z = 0.02$  (solar metallicity; solid lines) and  $Z = 0.008$  (dashed lines) of masses between 1 and  $3 M_{\odot}$  are also shown.

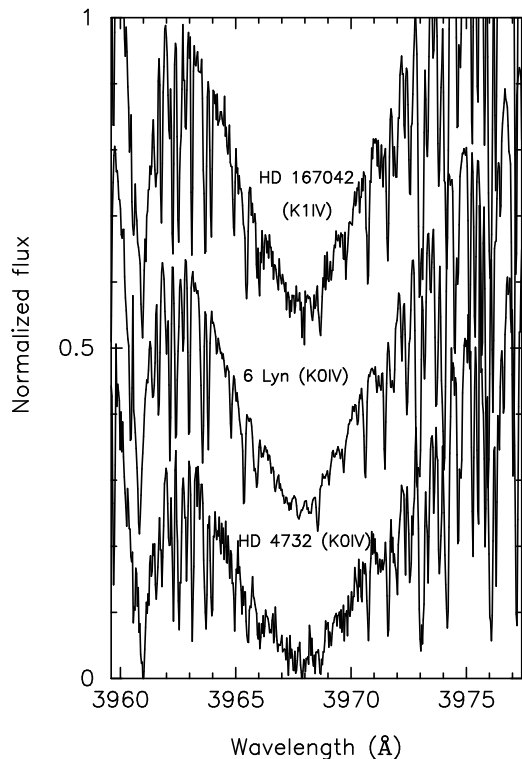


Fig. 2.— Spectra in the region of Ca H lines. Stars with similar spectral type to HD 4732 in our sample are also shown. A vertical offset of about 0.3 is added to each spectrum.

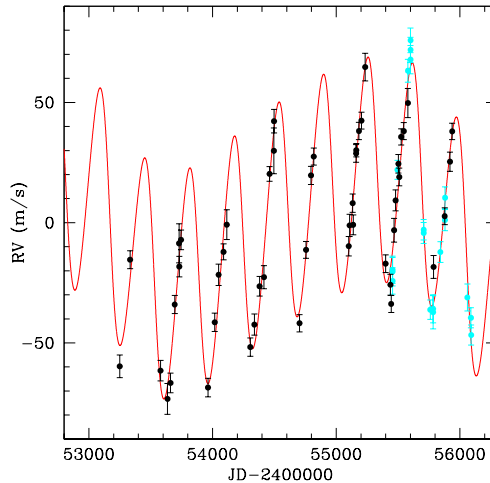


Fig. 3.— Two-planet fit for HD 4732 radial velocities. The planets have periods of 360 and 2732 days, and the RMS about this fit is  $7.09 \text{ m s}^{-1}$ . OAO data are shown as filled black circles, and AAT data are filled cyan circles.

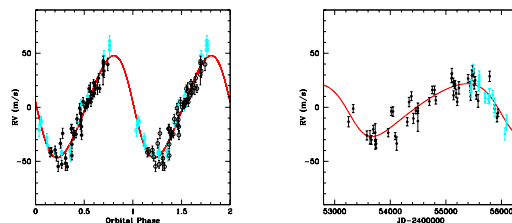


Fig. 4.— Left: Phase plot for HD 4732b ( $P = 360$  days), after removing the signal of the outer planet. Two cycles are shown for clarity. Right: Radial-velocity observations for HD 4732c ( $P = 2732$  days), after removing the signal of the inner planet. The symbols have the same meaning as in Figure 3.



TABLE 1  
 STELLAR PARAMETERS FOR HD 4732

Parameter	Value
Spectral Type	K0 IV <sup>a</sup>
$\pi$ (mas)	17.70±0.99
$V$	5.90
$B - V$	0.944
$A_V$	0.10
$M_V$	2.04
$B.C.$	-0.27
$T_{\text{eff}}$ (K)	4959±25 <sup>b</sup>
$\log g$ (cgs)	3.16±0.08 <sup>b</sup>
$v_t$ (km s <sup>-1</sup> )	1.12±0.07 <sup>b</sup>
[Fe/H] (dex)	0.01±0.04 <sup>b</sup>
$L$ ( $L_{\odot}$ )	15.5
$R$ ( $R_{\odot}$ )	5.4 (5.0–5.8) <sup>c</sup>
$M$ ( $M_{\odot}$ )	1.74 (1.60–1.94) <sup>c</sup>
$v \sin i_{\text{rot}}$ (km s <sup>-1</sup> )	1.45
$\sigma_{\text{HIP}}$ (mag)	0.006

<sup>a</sup>The star is listed in the Hipparcos catalogue as a K0 giant. But judged from the position of the star on the HR diagram (Figure 1), the star should be better classified as a less evolved subgiant.

<sup>b</sup>The uncertainties of these values are internal statistical errors (for a given data set of Fe I and Fe II line equivalent widths) evaluated by the procedure described in subsection 5.2 of Takeda et al. (2002).

<sup>c</sup>The values in the parenthesis correspond to the range of the values assuming the realistic uncertainties in  $\Delta \log L$  corresponding to parallax errors in the Hipparcos catalog,  $\Delta \log T_{\text{eff}}$  of  $\pm 0.01$  dex ( $\sim \pm 100$  K), and  $\Delta[\text{Fe}/\text{H}]$  of  $\pm 0.1$  dex.

TABLE 2  
 OAO RADIAL VELOCITIES FOR HD 4732

JD-2400000	Velocity ( $\text{m s}^{-1}$ )	Uncertainty ( $\text{m s}^{-1}$ )
53249.25552	-55.9	4.7
53333.01997	-11.6	3.7
53579.26965	-57.7	4.3
53636.21690	-69.4	6.4
53660.13539	-62.8	4.1
53693.98447	-30.2	3.8
53728.95697	-4.8	8.1
53730.93188	-14.4	4.3
53744.94607	-3.3	4.1
53963.26781	-64.7	3.8
54018.11973	-37.6	3.8
54049.02581	-17.8	4.4
54088.93606	-8.3	3.3
54114.88858	3.0	6.2
54305.29326	-47.9	3.8
54338.23288	-38.5	4.4
54380.15468	-22.6	4.1
54416.02081	-18.8	4.8
54460.93793	24.1	3.0
54495.89851	33.7	9.5
54496.90370	46.0	4.9
54703.25119	-38.0	3.6
54756.10553	-7.5	3.5
54796.00048	23.5	3.8
54817.94637	31.3	3.5
55101.16674	-5.9	4.0
55108.20638	2.7	4.6
55133.10162	11.9	3.8
55137.09148	2.9	4.1
55161.03266	32.6	3.7
55162.00982	34.0	2.8
55183.92889	42.0	3.6
55203.89392	46.3	3.5
55233.90048	68.5	5.8
55399.28930	-13.2	3.7
55438.17586	-22.0	4.4
55444.21320	-29.9	3.5
55468.16146	0.7	5.0
55480.13068	13.1	4.3
55503.02690	28.3	3.9
55510.06421	22.8	3.7
55524.97523	39.5	3.4
55546.92022	41.9	3.6
55579.91720	53.6	6.0
55787.29129	-14.6	4.8
55877.01304	6.5	3.5
55919.93294	29.2	4.0
55937.88506	41.8	3.4

TABLE 3  
AAT RADIAL VELOCITIES FOR HD 4732

JD-2400000	Velocity ( $\text{m s}^{-1}$ )	Uncertainty ( $\text{m s}^{-1}$ )
55455.16094	-19.7	5.6
55455.20587	-20.5	5.9
55456.06022	-24.3	5.5
55494.91653	21.9	4.0
55579.92330	63.1	4.8
55600.90903	67.7	5.9
55600.91897	75.7	5.1
55600.93330	71.8	5.3
55707.30755	-3.1	4.3
55707.31526	-4.4	4.4
55760.15572	-36.3	4.0
55783.13308	-37.3	6.9
55783.14079	-35.9	5.8
55841.99044	-12.3	4.3
55878.95827	1.0	4.4
55880.01556	10.3	4.5
56060.29762	-31.2	5.6
56089.30186	-39.6	4.2
56091.27740	-46.8	4.2

TABLE 4  
JITTER ESTIMATES

Added jitter ( $\text{m s}^{-1}$ )	$\chi^2_\nu$	RMS ( $\text{m s}^{-1}$ )
2.9	2.12	7.10
4.0	1.66	7.09
5.0	1.32	7.09
6.0	1.05	7.09
7.0	0.85	7.08
8.0	0.70	7.08
9.0	0.59	7.08
10.0	0.49	7.08

TABLE 5  
KEPLERIAN ORBITAL SOLUTIONS

Planet	Period (days)	$T_0$ (JD-2400000)	$e$	$\omega$ (degrees)	$K$ ( $\text{m s}^{-1}$ )	$m \sin i$ ( $M_{\text{Jup}}$ )	$a$ (AU)
HD 4732 b	$360.2 \pm 1.4$	$54967 \pm 18$	$0.13 \pm 0.06$	$85 \pm 16$	$47.3 \pm 3.5$	$2.37 \pm 0.34$	$1.19 \pm 0.05$
HD 4732 c	$2732 \pm 81$	$56093 \pm 103$	$0.23 \pm 0.07$	$118 \pm 15$	$24.4 \pm 2.2$	$2.37 \pm 0.38$	$4.60 \pm 0.23$

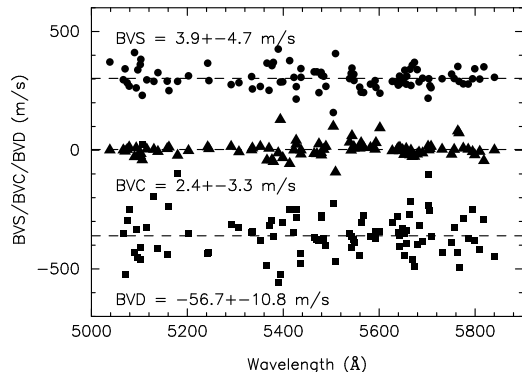


Fig. 5.— Bisector quantities of cross-correlation profiles between the templates of HD 4732 at phases with  $\sim 40 \text{ m s}^{-1}$  and with  $\sim -20 \text{ m s}^{-1}$  of the observed radial velocities: bisector velocity span (BVS, circles), bisector velocity curvature (BVC, triangles), and bisector velocity displacement (BVD, squares). Offsets of  $300 \text{ m s}^{-1}$  and  $-300 \text{ m s}^{-1}$  are added to BVS and BVD, respectively.

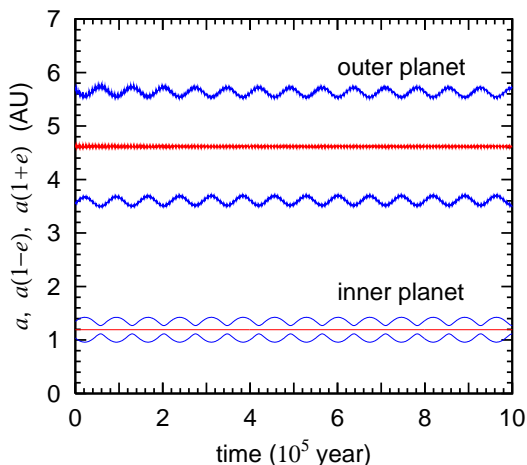


Fig. 6.— Evolution of semimajor axis  $a$ , pericenter  $a(1-e)$ , and apocenter  $a(1+e)$  distances for the two planets of HD 4732 system for the best-fit two-Keplerian model to the radial-velocity data. Red lines are for semimajor axis and blue ones are for pericenter (lower line for each planet) and apocenter (upper line for each planet) distance. We here assume  $i = 90^\circ$  and prograde coplanar orbits.

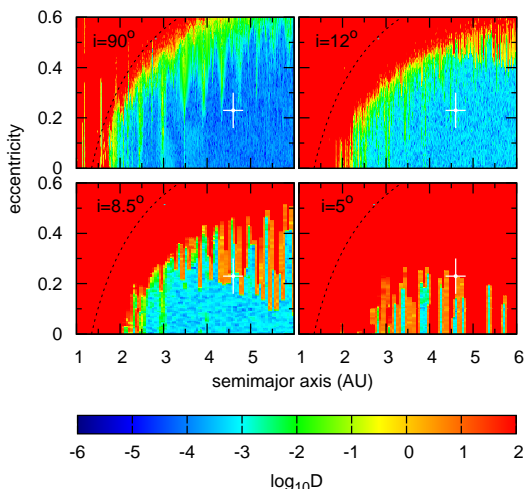


Fig. 7.— Stability map of the outer planet (HD 4732 c) for a coplanar prograde configuration with different values of inclination  $i$ . Orbital elements other than semimajor axis and eccentricity of the outer planet are taken from the best fit values. The color scale shows the level of mean motion diffusion,  $\log_{10} D$ . Blue to navy orbits are stable, while yellow to red orbits are chaotic. The step size of eccentricity is  $\Delta e = 0.005$ . The step sizes of semimajor axis are  $\Delta a = 0.005 \text{ AU}$  (top-left panel),  $\Delta a = 0.01 \text{ AU}$  (top-right panel), and  $\Delta a = 0.05 \text{ AU}$  (bottom panels). White crosses represent the best fitted  $a$  and  $e$  with their  $1 \sigma$  errors. Black dotted line is the orbit crossing line.